Check for updates

Multifunctional composite with hybrid carbon fiber and carbonaceous coconut particle reinforcement

Foster Feni[1], Maryam Jahan[2], Rong Zhao[3], Guoqiang Li[1,4], Guang-Lin Zhao[3] and Patrick F. Mensah[1]*

[1]Mechanical Engineering Department, Southern University and A&M College, Baton Rouge, LA, United States, [2]Chemistry Department, Southern University and A&M College, Baton Rouge, LA, United States, [3]Physics Department, Southern University and A&M College, Baton Rouge, LA, United States, [4]Department of Mechanical and Industrial Engineering, Louisiana State University, Baton Rouge, LA, United States

The utilization of multifunctional composite materials presents significant advantages in terms of system efficiency, cost-effectiveness, and miniaturization, making them highly valuable for a wide range of industrial applications. One approach to harness the multifunctionality of carbon fiber reinforced polymer (CFRP) is to integrate it with a secondary material to form a hybrid composite. In our previous research, we explored the use of carbonaceous material derived from coconut shells as a sustainable alternative to inorganic fillers, aiming to enhance the out-of-plane mechanical performance of CFRP. In this study, our focus is to investigate the influence of carbonized coconut shell particles on the non-structural properties of CFRP, specifically electromagnetic interference (EMI) shielding, thermal stability, and water absorption resistance. The carbonized material was prepared by thermal processing at 400 °C. Varying proportions of carbonized material, ranging from 1% to 5% by weight, were thoroughly mixed with epoxy resin to form the matrix used for impregnating woven carbon fabric with a volume fraction of 29%. Through measurements of scattering parameters, we found that the hybrid composites with particle loadings up to 3% exhibited EMI shielding effectiveness suitable for industrial applications. Also, incorporating low concentrations of carbonized particle to CFRP enhances the thermal stability of hybrid CFRP composites. However, the inclusion of carbonized particle to CFRP has a complex effect on the glass transition temperature. Even so, the hybrid composite with 2% particle loading exhibits the highest glass transition temperature and lowest damping factor among the tested variations. Furthermore, when subjected to a 7-day water immersion test, hybrid composites with 3% or less amount of carbonized particle showed the least water absorption. The favorable outcome can be attributed to good interfacial bonding at the matrix/fiber interface. Conversely, at higher particle concentrations, aggregation of particles and formation of interfacial and internal pores was observed, ultimately resulting in deteriorated measured properties. The improved non-structural functionalities observed in these biocomposites suggest the potential for a more sustainable and cost-effective

alternative to their inorganic-based counterparts. This advancement in multifunctional composites could pave the way for enhanced applications of biocomposites in various industries.

1 Introduction

The increasing use of multifunctional composite materials in industries such as aerospace, automobile, and electronics is driven by their economic benefits and desirable properties. These materials are designed not only for load-bearing functions like stiffness, strength, and toughness but also for other non-structural roles like self-healing, sensing, and actuation (Gibson, 2010). By integrating non-structural functionalities directly into the material, the need for additional components that could add weight and volume is eliminated, leading to improved overall efficiency (Narayana and Gupta Burela, 2018).

Carbon fiber reinforced polymer (CFRP) is highly sought after in aerospace, automobile, and other engineering applications for its high specific strength and stiffness, lightweight, corrosion resistance, and durability (Forintos and Czigany, 2019). To overcome the shortcomings such as low off-axis behavior, poor electrical and thermal conductivity of fiber reinforced composites (Pozegic et al., 2016; Ulus et al., 2016), these composites are often integrated with multiscale powders, including graphene, Al_2O_3, SiO_2, and Carbon Nanotubes (CNT) (Zheng et al., 2005; Cheng et al., 2009; Boroujeni et al., 2014; Mohanty and Srivastava, 2015). The addition of such particulates not only increases the toughness of the matrix but also enhances the matrix-fiber adhesion bond, leading to improved structural performance in the resulting hybrid composite. Nonetheless, their high cost and abrasiveness to processing tools is undesirable. In contrast, biomaterials offer advantages in terms of environmental friendliness, availability, and cost-effectiveness over their inorganic counterparts (Priya et al., 2023). Moreover, using agricultural waste in polymer-based composites for various applications is suitable for promoting a circular economy and sustainable environment (Taurino et al., 2023). Among the various available bio-based materials, coconut shell particles have shown promising results as a biofiller for enhancing the mechanical properties of polymers (Agunsoye et al., 2019; Mark et al., 2020) and non-structural properties, including the use as electrode catalyst in fuel cells (Jahan and Feni, 2022). Given their abundance in tropical areas and high carbon content with low O/C and H/C ratios, coconut shells hold great potential as biofillers (Prauchner and Rodríguez-Reinoso, 2012). However, the hydrophilic nature of coconut shells and other plant-based fillers, rich in hydroxyl groups, poses challenges when used in hydrophobic polymer matrices, leading to poor adhesion, and subsequently compromising structural performance and resistance to water absorption (Essabir et al., 2016a; Essabir et al., 2016b; Chougan et al., 2023). Water absorbed reduces the adhesion between the fiber and matrix by breaking the strong interfacial bond between the constituents. In the event of long exposure time, the reinforced material can absorb a large amount of water that causes swelling of

matrix, leading to debonding and deterioration of functionalities—one such is that the transfer of load from matrix to fiber is less effective compared to the original sample before water exposure (Sallal, 2014).

The process of carbonization has proven effective to circumvent the shortcomings of organic fillers. In our previous studies, we used carbonized particle from coconut shells as reinforcement to fabricate a hybrid composite. The resulting composite demonstrated improved tensile, flexural, and impact behavior compared to a control CFRP. While the primary use of CFRP in engineering applications lies in its structural superiority, exploring its potential for non-structural functionalities becomes crucial, especially when combined with hybrid reinforcements. In the aerospace and defense industry, properties like microwave absorption and hygrothermal stability are of particular interest. Microwave-absorbing capabilities are essential to ensure material reliability and act as shielding barriers against electromagnetic waves. Also, hygrothermal stability is critical to maintain material functionality and properties under varying temperature and moisture conditions during extended service conditions.

Although CFRP composites are known for their electromagnetic interference shielding applications, their potential for microwave absorption is yet to be fully developed (Qin and Brosseau, 2012). Electromagnetic interference (EMI) shielding is of utmost importance to prevent electronic devices and equipment from being affected by external electromagnetic signals or signals generated by neighboring components (Wang et al., 2013). EMI shielding continues to be a significant issue because of the rapid development of the electronic industry and products. Polymer-based conductive composites have emerged as a popular alternative to traditional metal-based shielding materials due to their unique advantages, including high specific strength, light weight, stable chemical properties, and ease of fabrication (Pradhan et al., 2020; Song et al., 2021; Wang et al., 2021). Shielding effectiveness (SE) is used to express the degree of attenuation of EM waves. Schelkunoff's theory, proposes that, some EM waves are directly reflected (SE_R) due to impedance mismatch when propagating along the shielding material's surface. The remaining EM waves are attenuated by the material as absorption loss (SE_A) and multiple reflection loss (SE_M), respectively. SE_M can typically be disregarded when SE_A is greater than 10 dB. Eq. 1 represents the total SE (SE_T) as follows (Zeng et al., 2020):2

$$SE_T = SE_R + SE_A \qquad (1)$$

It should be noted that the SE_A in the shield is not affected by the kind of EM waves; instead, it is substantially influenced by the shield's thickness, natural frequency, conductivity, and permeability. The SE_A of the EMI shielding increases with increasing thickness,

FIGURE 1
Schematic image illustrating the synthesis process of carbonized particle from coconut shells.

natural frequency, conductivity, and permeability. The most common materials being explored for EMI shielding spans various forms of carbon materials including graphene, CNT, carbon black, and other nanomaterials like MXene, nitride, sulfide, and carbide (Thomassin et al., 2013; Meng et al., 2018; Gupta and Tai, 2019; Zeng et al., 2020).

In summary, while our previous research confirmed the effectiveness of carbonized coconut shell particles in enhancing the mechanical performance of CFRPs, their influence on non-structural functionalities, particularly hygrothermal behavior and EMI shielding, remains unexplored. This constitutes a primary focus of our present study. Moreover, given the well-known high water absorption rates associated with cellulosic fillers due to their hydrophilic nature, it is imperative to ascertain the success of the carbonization process in mitigating these inherent weaknesses. Our second objective is to assess the water absorption resistance in our CFRP-biocomposites. The investigation of non-structural properties and water absorption resistance is vital to validate the practical applicability of CFRP-carbonized particle composites. Our research methodology involves EMI shielding assessment through scattering parameters and thermal behavior analysis using thermogravimetric and dynamic mechanical analysis, along with a 7-day water immersion test.

2 Materials and methods

2.1 Materials

Aero-Marine 300/21 epoxy system, sourced from Aeromarine Products Inc. was used as matrix; its favorable characteristics, including ease of processing, chemical resistance, high strength, and durability makes it suitable for composite fabrication. The reinforcement used was 3K tow plain weave carbon fiber from FiberGlast Corporation (Ohio, USA), known for its lightweight and high-strength properties, making it an ideal candidate for aerospace structures. The Carbonized Coconut Shell Particle (CCSP) was synthesized by heating clean coconut shells acquired from a local market (Walmart, USA) in an electrothermal furnace at $400°C$ for 2 h using a previously reported method (Feni et al., 2022). Figure 1 shows a schematic of the synthesis process for carbonized particle from coconut shells.

Energy dispersive analysis (EDS) conducted on the coconut powder both before and after carbonization revealed a notable increase in carbon content, along with a significant reduction in oxygen and nitrogen content after the carbonization process (Supplementary Figure S1).

2.2 SEM characterization

A sectioned surface of the hybrid composite was analyzed after fabrication. Hybrid composites with 3% and 5% particle loading were sectioned and coated with 5 nm iridium to make the surface conductive. A high-resolution Quanta 3D FE SEM/FIB dual system was used in analyzing the matrix-fiber interface by employing an electron accelerating voltage of 5 kV and 0.40 nA current.

2.3 XPS characterization

X-ray photoelectron spectroscopy was performed on precursor coconut before and after carbonization using Kratos analytical axis 165 to obtain information on elemental distribution. Using Al Kα X-ray beam, with a passing energy of 160 eV and 10 mA current, electron spectra of C–1s, N–1s, O–1s was collected and analyzed.

2.4 Composite fabrication

Hybrid composites with varying amounts of carbonized particle from 1% to 5% weight compositions were fabricated using woven carbon fabric with volume fraction fixed at 29%. For each hybrid composite, the required amount of carbonized particle was thoroughly mixed with aeromarine 300 epoxy resin by mechanically stirring to achieve homogeneity. The hardener was later added and stirred using a glass rod to obtain a uniform mixture. The mixture which now forms the matrix was used to impregnate the carbon fiber. The mold with the composite material was placed under pressure during curing process for 48 h. A control CFRP composite was fabricated using the same method and fiber volume fraction; however, in this case, the matrix comprises only epoxy resin and hardener without carbonized particle. A complete stepwise procedure is shown in Supplementary Figure S2.

2.5 Electromagnetic shielding characterization

To examine the EMI shielding characteristics of the samples, the scattering parameters (S-parameters) were measured in the frequency range of 1–26.5 GHz, using a coaxial transmission line method with an Agilent Network Analyzer N5230C PNA-L. The samples for analysis were 2 mm thick and fashioned into O-ring shapes with an outer diameter of 3.5 mm and an inner diameter of 1.5 mm for measurement purposes (Supplementary Figure S3).

2.6 Thermal analysis

2.6.1 Thermogravimetric analysis (TGA)

Thermogravimetric Analysis (TGA) was used to analyze composites' thermal stability, which is essential in determining their operating temperatures. An STA 7300 Thermal Analysis System from RTI laboratories was used to analyze each specimen with an average weight of 20 mg. Each sample was analyzed by heating from room temperature to 550°C at a ramp rate of 10°C/min.

An inert environment was created by argon gas flow at 150 mL/min. Data on weight loss with respect to temperature was collected.

2.6.2 Dynamic mechanical analysis (DMA)

DMA (Dynamic Mechanical Analysis) is a thermomechanical characterization technique used to measure the viscoelastic properties of polymeric materials. It provides valuable insights into a material's stiffness and damping properties as it undergoes deformation under the application of dynamic loads. The DMA analysis in this study was conducted using an RSA-G2 DMA instrument from TA Instruments. Rectangular specimens with a thickness of 2 mm and a width of 12 mm were used, and the measurements were performed on a 40 mm span length three-point bending fixture. To obtain the viscoelastic data, a temperature ramp was applied from room temperature to 110°C, with a ramp rate of 2°C/min and a testing frequency of 1 Hz, according to ASTM D7028.

## 2.7 Water absorption test

Exposure to moisture and water absorption affects mechanical properties including toughness, stiffness, and strength. Water absorption test was performed using rectangular specimens with a cross-sectional dimension of 25.4 mm × 2 mm, and 50 mm length. The samples were first dried in an oven at 50°C for 24 h and then placed in a desiccator for another 24 h per ASTM D570 (ASTM, 2014). The weight of specimens was taken to the nearest 0.001 g and quickly immersed in a beaker with distilled water at a temperature of 23°C for 7 days. After 24 h, each specimen is taken out of the water, surface wiped completely with absorbent paper, and quickly weighed. The specimen is immersed back into the water, and the process is repeated every 24 h. The water absorption in percentage is calculated by the expression below, where w_1 and w_o are the weight after and before immersion.

$$\% \text{ Water Absorption} = \frac{W_1 - W_0}{W_0} \times 100\%$$

3 Results and discussions

3.1 SEM characterization

The analysis of matrix-fiber interfacial bonding was conducted using scanning electron microscopy. In Figure 2A, we observe the interfacial behavior of hybrid composites with a 3% carbonized particle loading. At this particle loading, the carbonized particles effectively contribute to toughening the epoxy, resulting in improved bond strength at the matrix-fiber interface. This is clearly evidenced by the strong interfacial bonding shown in Figure 2A, where no visible voids or pores are apparent at this level of magnification. However, when the particle loading is increased to 5%, the carbonized particles tend to aggregate, forming clusters within the matrix, as depicted in Figure 2B. These particle clusters become lodged between the fibers, leading to inadequate wetting and bonding. Additionally, internal microvoids are distributed within the composite. Images captured at different locations in the hybrid composite with 5% particle loading (see

FIGURE 2
SEM image of hybrid composite with **(A)** 3% and **(B)** 5% particle loading.
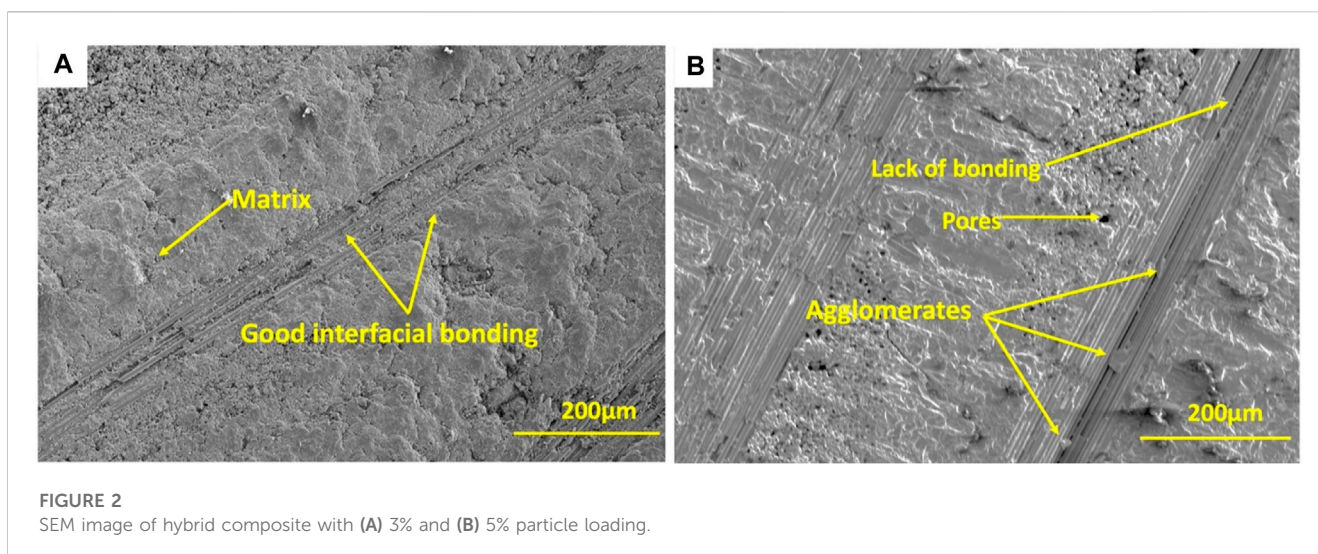
Supplementary Figure S4) reveal significant interfacial pores and an internal pore with an approximate diameter of 69 μm. These pores can have a substantial impact on the mechanical, hygrothermal, and other properties of the composite.

The investigation into the change in elemental distribution on the surface of the coconut shell sample before and after carbonization was conducted using X-ray photoelectron spectroscopy (XPS) analysis. The primary elements present in both samples were found to be carbon (C), oxygen (O), and nitrogen (N) (Figure 3A, B). As shown in the inserted table of Figure 3A, B, the percentage of carbon increases, while the percentages of oxygen and nitrogen decrease upon carbonization.

The C1s spectra for both the raw (precursor) coconut and CCSP samples (Figure 3C, D) exhibited three major peaks with approximate binding energies occurring at 288.5, 286, and 285 eV, which can be attributed to C=O, C–O, and C–C functional groups, respectively (Li et al., 2017). In the raw coconut shells, the percentage of C=O, C–O, and C–C functional groups were measured to be 65.06%, 23.92%, and 11.03%, respectively (Figure 3C). However, in the carbonized sample, the proportion of these functional groups shifted to 15.37%, 39.99%, and 44.65%, respectively (Figure 3D). This shift indicates an increase in the percentage of C–C bonds and a decrease in oxygen-containing functional groups, such as C=O and C–O, after carbonization. Additionally, the intensity of the C1s peak for CCSP (25,000 cps) was approximately 1.8 times higher than that of the raw (precursor) coconut (14,000 cps). The reduction in oxygen-containing functional groups present in cellulose, hemicellulose, and lignin, and the increase in carbon content after carbonization are desirable for enhancing surface compatibility and water absorption resistance.

The O1s XPS spectra of raw coconut shells (Figure 3E) displayed two major peaks occurring at around 533.5 and 531.5 eV binding energies, which corresponds to C=O and O–C=O functional groups, respectively (Li et al., 2016). For the raw coconut sample, the proportions of C=O and O–C=O are 40.23% and 59.77%, respectively. On the other hand, in the carbonized sample, the proportion of C=O is 100%, and the O-C=O peak was completely eliminated (Figure 3F). Furthermore, the intensity of O1s for raw coconut shells (22,000 cps) is almost twice that of the CCSP sample (12,000 cps). The reduction in oxygen content in

CCSP is due to the carbonization process upon heating. The elemental composition analysis from EDS also confirmed similar results (Supplementary Figure S1).

3.2 Electromagnetic shielding

The S parameters, denoted as Sij, indicate the transmission of electromagnetic waves from port j to port i. They are commonly employed to classify various types of shielding materials. Eqs. 2-4 utilize these S parameters to determine the reflectance rate (R), absorption rate (A), and transmittance rate (T) (Zhao et al., 2022):

$$R = |S_{11}|^2 \, (or \, |S_{22}|^2) \qquad (2)$$

$$T = |S_{21}|^2 \, (or \, |S_{12}|^2) \qquad (3)$$

$$A = 1 - R - T \qquad (4)$$

Figure 4 presents the EMI shielding effectiveness (SE_T) of the composites with varying loadings of CCSP across the frequency range from 1 to 26.5 GHz. The composite samples in the figure have a thickness of 2 mm. In general, SE_T values ≤10 dB indicate ineffective shielding, while values between 10 and 30 dB are considered acceptable for EMI shielding effectiveness. For industrial and commercial applications requiring a minimum shielding effectiveness of 20 dB, a value of $SE_T \geq 30$ dB is considered to be beyond the acceptable range. The SE_T of the composite with no CCSP loading is higher than that of the other CCSP loaded. It shows SE_T of 23–46 dB in the frequency range of 1–26.5 GHz, with a maximum value of 46 dB observed at 26.5 GHz. With an increase in CCSP loading from 1% to 3%, the SE_T of the composites remains consistent at approximately 20 dB within the frequency range of 1–10 GHz and exceeds 20 dB within the frequency range of 10–26.5 GHz. For the composites with 4% CCSP loading, the SE_T is between 13 dB and 20 dB at the frequency range of 1–15 GHz, increasing gradually from 20 dB to 35 dB in the range of 15–26.5 GHz. When the loading of CCSP reaches 5%, the SE_T of composites falls below 20 dB in most of the frequency range measured. The EMI shielding performance of the composites is strongly influenced by their electrical properties, particularly their electrical conductivity, which is known to have a significant impact on microwave attenuation. In this
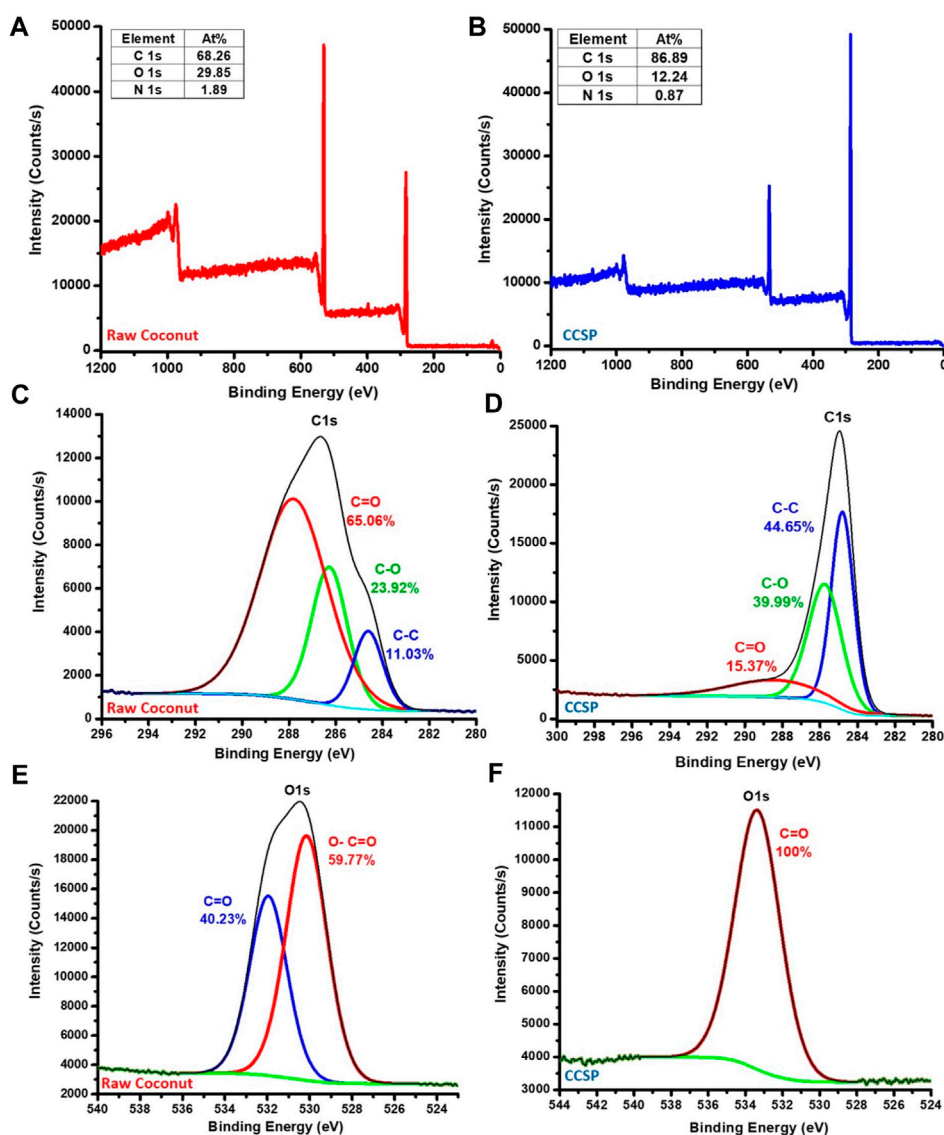
FIGURE 3
XPS diagram of Raw coconut particles and Carbonized Coconut Shell Particle (CCSP). **(A)** Survey of the present elements and element content percentages in Raw coconut particles. **(B)** Survey of the present elements and element content percentages in CCSP. **(C)** C1s XPS spectra of Raw coconut particles. **(D)** C1s XPS spectra of CCSP. **(E)** O1s XPS spectra of Raw coconut particles. **(F)** O1s XPS spectra of CCSP.

study, the high-conductivity carbon fiber formed the electrical networks of the composites, while CCSP had significantly lower conductivity. A high loading of CCSP in the composite could weaken some of the electrical networks, leading to reduced conductivity (Li et al., 2020). Moreover, the increased viscosity of the CCSP-epoxy solution with CCSP loading resulted in rough surface grains that could decrease reflections, resulting in lower SE_T values.
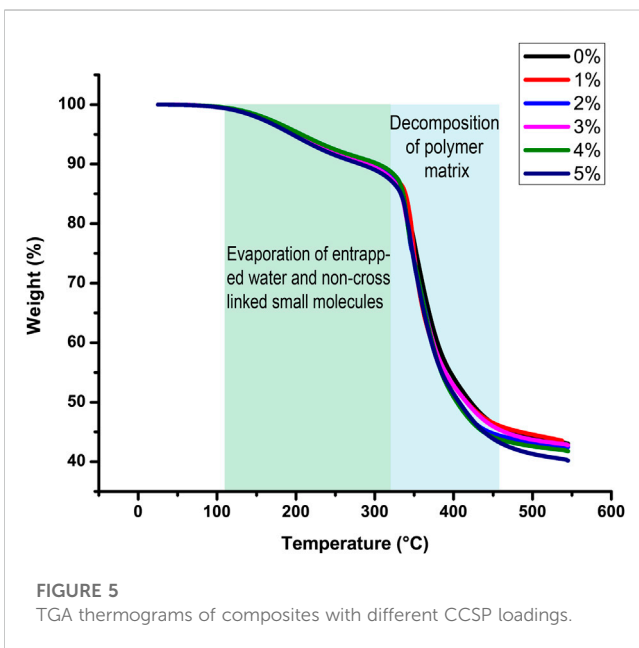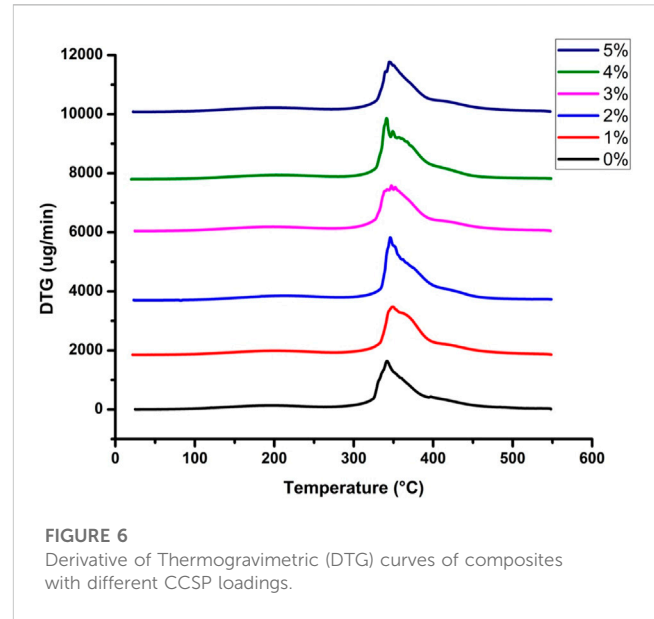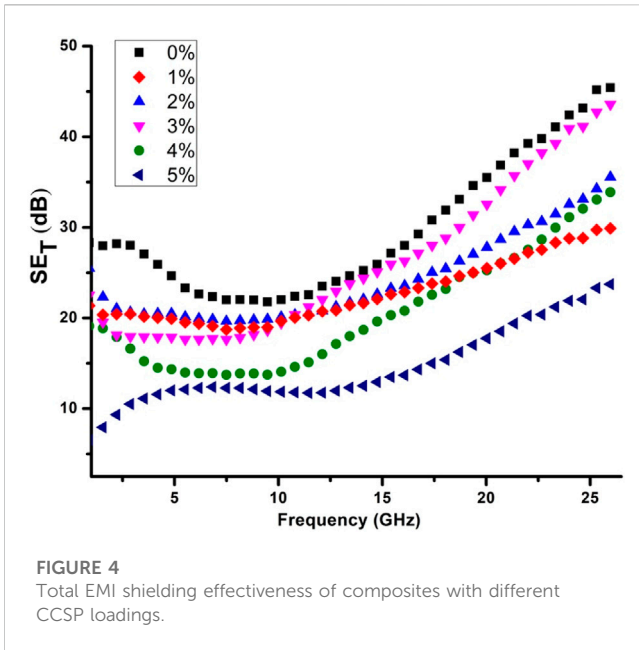
3.3 Thermal analysis

3.3.1 Thermogravimetric analysis

Thermogravimetric analysis (TGA) is a widely used method for analyzing the moisture and volatile components in materials, as they can act as precursors in deteriorating the mechanical and thermal

performance of the materials. Figure 5 presents the TGA analysis result showing percent weight loss with respect to temperature for each composite with varying amount of carbonized particle.

The reference and hybrid composites undergo a two-stage decomposition between 25°C and 550°C. The first decomposition stage is a slight decomposition occurring between 120°C and 300°C—this may be attributed to the uncrosslinked small molecules and vaporization of moisture entrapped through dehydration of secondary alcoholic group present in epoxy (Khan et al., 2020). Beyond this point, enough heat has been absorbed to initiate the degradation of the sample, and this occurs between 305°C and 450°C where a sharp drop of the curve is observed. This indicates the complete degradation of epoxy matrix and its components (Rezaei et al., 2009).

The decomposition behavior in the second degradation stage of the composites, 300°C–450°C, was used in evaluating the thermal

FIGURE 4
Total EMI shielding effectiveness of composites with different CCSP loadings.

FIGURE 6
Derivative of Thermogravimetric (DTG) curves of composites with different CCSP loadings.

FIGURE 5
TGA thermograms of composites with different CCSP loadings.

increased by 5°C in both 1% and 2% CCSP composites and by 7°C in that with 3% CCSP. In other words, the temperature required to degrade the hybrid CFRP composites with CCSP is slightly higher than that without CCSP. The improved thermal stability at lower particle loadings can be attributed to good particle dispersion in epoxy, providing a solid interaction at the fiber-matrix interface (Mohanty and Srivastava, 2015; Suchitra and Renukappa, 2016). Good dispersion and interfacial bonding restrict the molecular movement and diffusion of volatiles in the matrix (Nagaraja et al., 2022). The TGA results provide strong evidence that our hybrid biocomposites exhibit thermal stability on par with traditional CFRPs, indicating their functionality within practical temperature ranges. This finding addresses a critical limitation associated with cellulosic biofillers—their inherently poor thermal properties, primarily stemming from their composition. On the other hand, the lower decomposition temperature at higher particle loadings can be explained by the aggregation of CCSP in the matrix (Supplementary Figure S4), which compromises the thermal integrity of these composite panels (Mohanty and Srivastava, 2015). The agglomeration of particles leads to reduced interfacial bonding, allowing for easier diffusion of volatile components and resulting in lower thermal stability for composites with higher CCSP loadings.

3.3.2 Dynamic mechanical analysis

CFRP is expected to exhibit viscoelastic properties due to its polymer component. Dynamic Mechanical Analysis (DMA) is a technique that allows the simultaneous analysis of the elastic and viscous response of the composite panels through an oscillatory experiment, measuring the phase shift. The stress response is decoupled into two parts: the storage modulus and the loss modulus. The storage modulus represents the energy stored elastically as load is applied, and it relates to the elastic part of the material. The loss modulus measures the energy lost under stress, which is related to the viscous component of the composite and describes its ability to dampen energy through heat generation (Supplementary Figure S5).
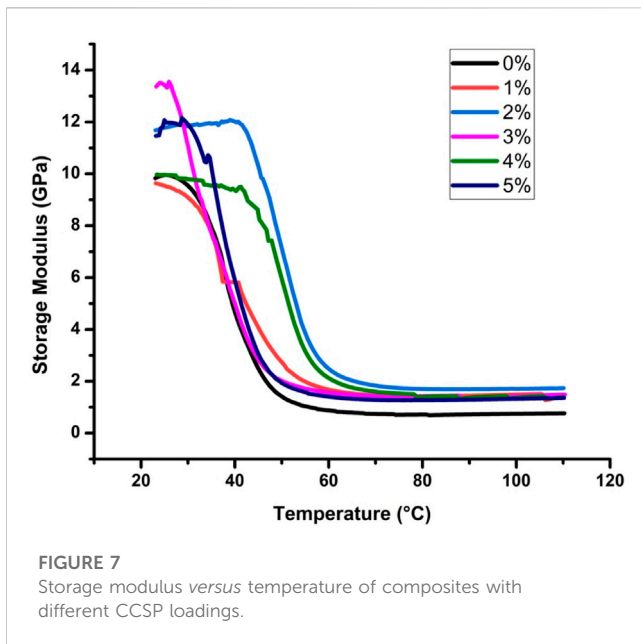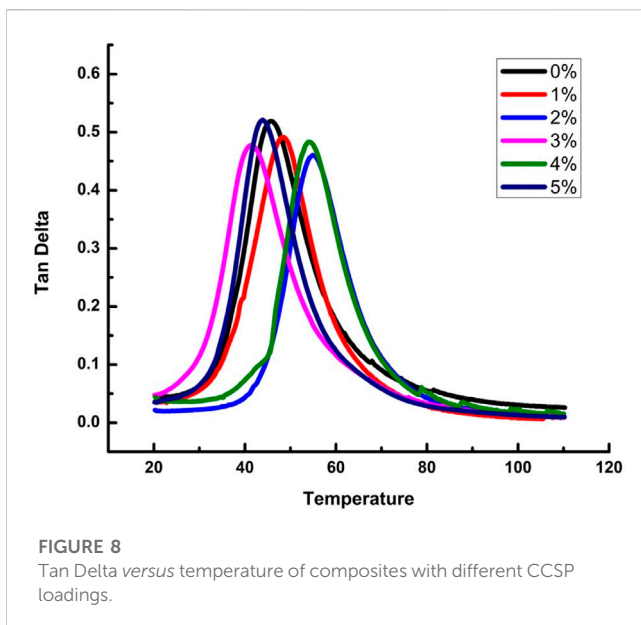
stability, as the slight weight loss from moisture is similar for all composites. To obtain the decomposition and initial degradation temperature, a curve of derivative of weight loss with change in temperature, generally called derivative of thermogravimetry (DTG) was used as shown in Figure 6. The temperature at the peak of this curve is considered the decomposition temperature, while the temperature at which the composite starts to degrade is the initial decomposition temperature (IDT) (Zhou et al., 2007; Chowdhury et al., 2018).

The incorporation of lower proportions of carbonized particles up to 3% slightly increases the IDT and decomposition temperature of the hybrid biocomposites compared to the reference composite, hence increased thermal stability. The decomposition temperature is

FIGURE 7
Storage modulus *versus* temperature of composites with different CCSP loadings.

FIGURE 8
Tan Delta *versus* temperature of composites with different CCSP loadings.

Figure 7 shows the effect of temperature on the storage modulus of the composites with varying concentrations of CCSP. It is observed that the elastic modulus of the biocomposites is higher than that of the bare CFRP. The storage modulus is maximum at a lower temperature and then begins to decrease with increasing temperature, particularly close to the glass transition zone. This reduction in storage modulus is a result of the viscoelastic nature of the polymer composite at this point. The storage modulus is dependent on temperature, meaning the higher the glass transition temperature (T_g), the higher the temperature and time at which the material loses its storage modulus (Chaudhary et al., 2018). This trend is evident in the storage modulus curve of the hybrid composites with 2% and 4% CCSP, which exhibit higher glass transition temperature (Supplementary Figure S5; Figure 8); These

composites take longer to lose their storage modulus compared to reference CFRP and 5% CCSP composite.

The resulting tan delta curve for each composite panel with different particle loading is shown in Figure 8. Tan delta describes the energy dissipation or damping behavior of a material and is derived as a ratio of loss modulus to storage modulus. The temperature at the peak of tan delta curve gives the glass transition temperature (O'Donnell et al., 2004). Glass transition also referred as α-transition is a reversible transition of most polymeric materials between a rubbery state and hard glassy state. The temperature at which this happens is considered as glass transition temperature, T_g (Reddy and Reddy, 2014).

As seen in Figure 8, tan delta is at its minimum at room temperature for all composites and increases as temperature increases before attaining a maximum at glass transition temperature. It then decreases in the rubbery state with increasing temperature. Damping behavior is generally low at a temperature below T_g because chain segments are frozen and immobile in this temperature range. The deformation at this point is mainly elastic, and molecular slip from viscous flow is restricted. Also above T_g, chain segments are mobile, and resistance to flow is less, hence, low damping (Reddy and Reddy, 2014). Damping behavior provides information about the elastic and non-elastic behavior of a material, where a high damping capability suggests a highly non-elastic material, and a low damping capability indicates an elastic nature (Saba et al., 2016). Addition of carbonized particle to the matrix (epoxy) of CFRP lowers the tan delta peak (Figure 8). The high tan delta peak of the reference CFRP without CCSP indicates a more viscose composite. Incorporating CCSP increases the CFRP's elasticity, hence the lower damping factor.

From Figures 7, 8; Supplementary Figure S5, it is evident that the effect of CCSP concentration on the viscoelastic properties, particularly Tg of composite panels, is complex and involves several competing events within the composite. On one hand, CCSP may act as "bearings," facilitating the motion of polymeric chains or segments, which lowers the Tg. Additionally, the incorporation of CCSP may interrupt the growth of the polymeric network during the curing process, further reducing the Tg. On the other hand, strong interfacial bonding between the polymer matrix and the CCSP particles and carbon fiber can limit the mobility of the polymeric chains and segments, leading to an increase in T_g (Vilay et al., 2008; Man et al., 2009; Raghavendra et al., 2013; Atiqah et al., 2018; Mahesh Babu and Venkateswara Rao, 2018). The final T_g of the composite results from the combination of these competing factors. It is worth noting that several repetitions of the DMA test were conducted, yielding similar results. However, further in-depth studies are necessary to better understand the underlying mechanisms behind these complex behaviors.

3.4 Water absorption test results

Figure 9 presents the percentage of weight gained by each composite sample at different immersion times during the 7 days of water exposure. Water absorption increases steadily in all samples until a saturation point is observed in the reference CFRP, 1%, and 2% hybrid composites after 144 h. The percentage of water absorbed

FIGURE 9
Percentage weight gained by composites at different immersion time.
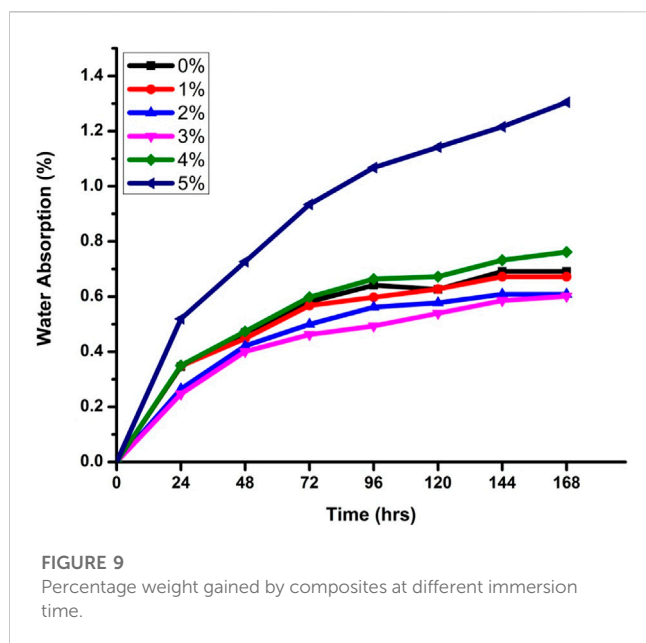
in hybrid composites with 1%, 2%, and 3% particle loadings is lower than that of the bare composite for each 7-day immersion period. This improvement in water resistance can be attributed to the good interfacial bond resulting from the proper dispersion of CCSP. The strong interfacial adhesion between epoxy and particles, as well as between the matrix and fibers, leads to a denser interfacial region. As a result, the diffusion of water molecules is slowed down due to the reduced availability of free pores at the interface for water penetration (Raghavendra et al., 2013; Mahesh Babu and Venkateswara Rao, 2018). Past research showed a reduction in the diffusion coefficient of epoxy reinforced with inorganic particles compared to neat epoxy after water absorption test at room temperature (Kalil, 2013). It is worth mentioning that the testing was conducted over a period of days, and it is possible that properties may vary with longer immersion durations. Nevertheless, when observing the water absorption rate between the sixth and seventh days for 1%, 2%, and 3% hybrid composite, which remained nearly constant, we anticipate only a slight increase or possibly the maintenance of this rate. This expectation is logically supported by the minimal presence of pores in the SEM image of the hybrid composite with a 3% loading CCSP. Any existing pores would likely be saturated, given the driving force necessary for capillary action.

However, at higher CCSP loadings of 4% and 5%, the composite's moisture absorption increases. The high-water absorption at higher particle loadings can be attributed to the agglomeration of particles, which deteriorates the adhesion between the matrix and reinforcement. The formation of microvoids and cracks at the interface, increases the capillary action hence high water absorption (Supplementary Figure S4). Similar findings were observed by Oluyemi et al. (Daramola and Akintayo, 2018), here epoxy reinforced with higher loadings of green silica particles obtained from rice husk ash exhibited higher water absorption due to particle aggregation. Given the consistent absorption rate observed between day 4 and day 7 in the 4% and 5% hybrid composites, it can be inferred that the absorption rate will continue to rise for a period before reaching saturation.

At the end of the 7-day period, the hybrid composite with 3% CCSP loading shows the least weight gain of 0.6%, while the one with 5% CCSP loading has the highest water absorption ratio of 1.3%. Previous studies on water absorption of polymers reinforced with untreated biofillers, in the form of both fibers and particles, have shown increased water absorption (Bhaskar and Singh, 2013; Singh, 2013; Sallal, 2014; Chandramohan and Presin Kumar, 2017). This is mainly due to the presence of cellulosic material containing hydroxyl group (-OH), which has a high affinity of bonding to water molecules and their incompatibility to form strong interfacial bonds (Vilay et al., 2008; Ashori and Nourbakhsh, 2010; Ashori and Sheshmani, 2010). In this work, the facile method of carbonization process effectively removes the cellulosic content, resulting in increased compatibility and reduced water absorption.

4 Summary and conclusion

In summary, our study focused on investigating the non-structural functionalities of hybrid biocomposites based on CFRP integrated with carbonized particles derived from coconut shells. We examined the electromagnetic interference (EMI) shielding, thermal behavior, and water absorption characteristics of these composites.

Our analysis of the scattering parameters revealed that the hybrid biocomposites exhibited excellent EMI shielding performance. Shielding effectiveness values exceeding 15 dB were achieved for composites containing 1%–3% carbonized coconut shell particle (CCSP) loadings in the frequency range of 10–26.5 GHz. This level of shielding effectiveness is deemed suitable for various industrial applications.

Through thermogravimetric analysis, we observed that the addition of low concentration of carbonized particles slightly increases the decomposition temperature of CFRP. However, from dynamic mechanical analysis, we observed a complex effect on the glass transition temperature of CFRP upon the inclusion of our carbonized material, possibly due to its double-edge effect. Furthermore, the incorporation of particles into CFRP enhanced the storage modulus of the hybrid composites.

We also assessed the water absorption resistance of the hybrid composites. It was found that composites with lower particle loadings exhibited improved resistance to water absorption compared to the reference CFRP. The water absorption decreased with increasing particle loading up to 3%. However, higher particle loadings deviated from this trend, with the composite containing 5% CCSP loading demonstrating the maximum absorption ratio.

In conclusion, the facile method of carbonization, achieved through heating, effectively eliminated the cellulosic content of the coconut shell. This process significantly enhances compatibility, resulting in improved thermal stability and resistance to water absorption. Our method eliminates the use of chemical treatments on cellulosic fillers that may pose environmental challenges or impact the inherent properties. In addition, our hybrid composites exhibited excellent EMI shielding performance and enhanced storage modulus. It is worth noting, however that, higher particle loadings can lead to detrimental property effects due to aggregation. These findings establish the multifunctionality of our bioparticle-CFRP hybrid composite, which presents a promising and sustainable

alternative to traditional inorganic particle-CFRP composites. While further analysis is necessary to fully understand the potential of these composites, they hold promise for practical applications in both the automobile and aerospace industries. These sectors prioritize considerations such as weight reduction and cost-effectiveness in their materials. Therefore, the performance enhancements observed in these hybrid CFRP-biocomposites, in addition to their sustainability make them attractive candidates for use in structural and non-structural components within these industries. Further research and testing will help determine the extent of their suitability and the specific applications where they can excel.

Data availability statement

The raw data supporting the conclusion of this article will be made available by the authors, without undue reservation.

Author contributions

FF: Conceptualization, Data curation, Investigation, Methodology, Writing–original draft, Formal Analysis. MJ: Conceptualization, Investigation, Supervision, Writing–review and editing, Formal Analysis. RZ: Investigation, Writing–review and editing, Methodology. GL: Writing–review and editing, Funding acquisition. G-LZ: Funding acquisition, Writing–review and editing, Investigation, Resources, Formal Analysis. PM: Funding acquisition, Resources, Writing–review and editing, Project administration, Supervision, Formal Analysis.

Funding

Conflict of interest

The authors declare that the research was conducted in the absence of any commercial or financial relationships that could be construed as a potential conflict of interest.

The author(s) declared that they were an editorial board member of Frontiers, at the time of submission. This had no impact on the peer review process and the final decision.

Publisher's note

All claims expressed in this article are solely those of the authors and do not necessarily represent those of their affiliated organizations, or those of the publisher, the editors and the reviewers. Any product that may be evaluated in this article, or claim that may be made by its manufacturer, is not guaranteed or endorsed by the publisher.

Supplementary material

The Supplementary Material for this article can be found online at: https://www.frontiersin.org/articles/10.3389/fmats.2023.1278222/full#supplementary-material

References

Agunsoye, J. O., Odumosu, A. K., and Dada, O. (2019). Novel epoxy-carbonized coconut shell nanoparticles composites for car bumper application. *Int. J. Adv. Manuf. Technol.* 102, 893–899. doi:10.1007/s00170-018-3206-0

Ashori, A., and Nourbakhsh, A. (2010). Reinforced polypropylene composites: effects of chemical compositions and particle size. *Bioresour. Technol.* 101, 2515–2519. doi:10.1016/j.biortech.2009.11.022

Ashori, A., and Sheshmani, S. (2010). Hybrid composites made from recycled materials: moisture absorption and thickness swelling behavior. *Bioresour. Technol.* 101, 4717–4720. doi:10.1016/j.biortech.2010.01.060

Astm, D. 570 (2014). Standard test method for water absorption of plastics. *ASTM Stand.* 98, 25–28.

Atiqah, A., Jawaid, M., Sapuan, S. M., Ishak, M., and Alothman, O. Y. (2018). Thermal properties of sugar palm/glass fiber reinforced thermoplastic polyurethane hybrid composites. *Compos Struct.* 202, 954–958. doi:10.1016/j.compstruct.2018.05.009

Bhaskar, J., and Singh, V. K. (2013). Water absorption and compressive properties of coconut shell particle reinforced-epoxy composite. *J. Mater. Environ. Sci.* 4, 113–116.

Boroujeni, A. Y., Tehrani, M., Nelson, A. J., and Al-Haik, M. (2014). Hybrid carbon nanotube-carbon fiber composites with improved in-plane mechanical properties. *Compos. Part B Eng.* 66, 475–483. doi:10.1016/j.compositesb.2014.06.010

Chandramohan, D., and Presin Kumar, A. J. (2017). Experimental data on the properties of natural fiber particle reinforced polymer composite material. *Data Brief.* 13, 460–468. doi:10.1016/j.dib.2017.06.020

Chaudhary, V., Bajpai, P. K., and Maheshwari, S. (2018). An investigation on wear and dynamic mechanical behavior of jute/hemp/flax reinforced composites and its hybrids for tribological applications. *Fibers Polym.* 19, 403–415. doi:10.1007/s12221-018-7759-6

Cheng, D. Q., Wang, X. T., Zhu, J., Qiu, D. h., Cheng, X. w., and Guan, Q. f. (2009). Friction and wear behavior of carbon fiber reinforced brake materials. *Front. Mater Sci. China* 3, 56–60. doi:10.1007/s11706-009-0012-5

Chougan, M., Ghaffar, S. H., and Al-Kheetan, M. J. (2023). Graphene-based nano-functional materials for surface modification of wheat straw to enhance the performance of bio-based polylactic acid composites. *Mater. Today Sustain.* 21, 100308. doi:10.1016/j.mtsust.2022.100308

Chowdhury, Z. Z., Krishnan, B., Sagadevan, S., Rafique, R., Hamizi, N., Abdul Wahab, Y., et al. (2018). Effect of temperature on the physical, electro-chemical and adsorption properties of carbon micro-spheres using hydrothermal carbonization process. *Nanomaterials* 8, 597–624. doi:10.3390/nano8080597

Daramola, O. O., and Akintayo, O. S. (2018). Water absorption characteristics of epoxy matrix composites reinforced with green silica particles. *Leonardo Electron. J. Pract. Technol.* 2018, 215–232.

Essabir, H., Bensalah, M. O., Rodrigue, D., Bouhfid, R., and Qaiss, A. (2016a). Structural, mechanical and thermal properties of bio-based hybrid composites from waste coir residues: fibers and shell particles. *Mech. Mater.* 93, 134–144. doi:10.1016/j.mechmat.2015.10.018

Essabir, H., Bensalah, M. O., Rodrigue, D., Bouhfid, R., and Qaiss, A. e. k. (2016b). Biocomposites based on Argan nut shell and a polymer matrix: effect of filler content and coupling agent. *Carbohydr. Polym.* 143, 70–83. doi:10.1016/j.carbpol.2016.02.002

Feni, F., Jahan, M., Dawan, F., Ibekwe, S., Li, G., and Mensah, P. (2022). Enhancing the mechanical performance of carbon fiber reinforced polymer using carbonized coconut shell particles. *Mater Today Commun.* 33, 104727. doi:10.1016/j.mtcomm.2022.104727

Forintos, N., and Czigany, T. (2019). Multifunctional application of carbon fiber reinforced polymer composites: electrical properties of the reinforcing carbon fibers – a short review. *Compos B Eng.* 162, 331–343. doi:10.1016/j.compositesb.2018.10.098

Gibson, R. F. (2010). A review of recent research on mechanics of multifunctional composite materials and structures. *Compos Struct.* 92, 2793–2810. doi:10.1016/j.compstruct.2010.05.003

Gupta, S., and Tai, N. H. (2019). Carbon materials and their composites for electromagnetic interference shielding effectiveness in X-band. *Carbon N. Y.* 152, 159–187. doi:10.1016/j.carbon.2019.06.002

Jahan, M., and Feni, F. (2022). Environmentally friendly bifunctional catalyst for ORR and OER from coconut shell particles. *Adv. Mater. Phys. Chem.* 12, 106–123. doi:10.4236/ampc.2022.125008

Kalil, A. (2013). The effect of particles as additives on water absorption for epoxy resin. *Int. J. Appl. or Innovation Eng. Manag. (IJAIEM)* 2, 131–136.

Khan, A., Asiri, A. M., Jawaid, M., Saba, N., and Inamuddin, (2020). Effect of cellulose nano fibers and nano clays on the mechanical, morphological, thermal and dynamic mechanical performance of kenaf/epoxy composites. *Carbohydr. Polym.* 239, 116248. doi:10.1016/j.carbpol.2020.116248

Li, K., Zhao, R., Xia, J., and Zhao, G. L. (2020). Reinforcing microwave absorption multiwalled carbon nanotube–epoxy composites using glass fibers for multifunctional applications. *Adv. Eng. Mater* 22, 1–7. doi:10.1002/adem.201900780

Li, Z., Hu, X., Xiong, D., Li, B., Wang, H., and Li, Q. (2016). Facile synthesis of bicontinuous microporous/mesoporous carbon foam with ultrahigh specific surface area for supercapacitor application. *Electrochim Acta* 219, 339–349. doi:10.1016/j.electacta.2016.10.028

Li, Z., Zhang, L., Li, B., Liu, Z., Liu, Z., Wang, H., et al. (2017). Convenient and large-scale synthesis of hollow graphene-like nanocages for electrochemical supercapacitor application. *Chem. Eng. J.* 313, 1242–1250. doi:10.1016/j.cej.2016.11.018

Mahesh Babu, S., and Venkateswara Rao, M. (2018). Effect of basalt powder on mechanical properties and dynamic mechanical thermal analysis of hybrid epoxy composites reinforced with glass fiber. *J. Chin. Adv. Mater. Soc.* 6, 311–328. doi:10.1080/22243682.2018.1470030

Man, Y. H., Li, Z. C., and Zhang, Z. J. (2009). Interfacial friction damping characteristics in MWNT-filled polycarbonate composites. *Front. Mater Sci. China* 3, 266–272. doi:10.1007/s11706-009-0040-1

Mark, U. C., Madufor, I. C., Obasi, H. C., and Mark, U. (2020). Influence of filler loading on the mechanical and morphological properties of carbonized coconut shell particles reinforced polypropylene composites. *J. Compos Mater* 54, 397–407. doi:10.1177/0021998319856070

Meng, F., Wang, H., Huang, F., Guo, Y., Wang, Z., Hui, D., et al. (2018). Graphene-based microwave absorbing composites: a review and prospective. *Compos B Eng.* 137, 260–277. doi:10.1016/j.compositesb.2017.11.023

Mohanty, A., and Srivastava, V. K. (2015). Effect of alumina nanoparticles on the enhancement of impact and flexural properties of the short glass/carbon fiber reinforced epoxy based composites. *Fibers Polym.* 16, 188–195. doi:10.1007/s12221-015-0188-5

Nagaraja, K. C., Rajanna, S., Prakash, G. S., and Rajeshkumar, G. (2022). Improvement of mechanical and thermal properties of hybrid composites through addition of halloysite nanoclay for light weight structural applications. *J. Industrial Text.* 51, 4880S–4898S. doi:10.1177/1528083720936624

Narayana, K. J., and Gupta Burela, R. (2018). A review of recent research on multifunctional composite materials and structures with their applications. *Mater Today Proc.* 5, 5580–5590. doi:10.1016/j.matpr.2017.12.149

O'Donnell, A., Dweib, M. A., and Wool, R. P. (2004). Natural fiber composites with plant oil-based resin. *Compos Sci. Technol.* 64, 1135–1145. doi:10.1016/j.compscitech.2003.09.024

Pozegic, T. R., Anguita, J. v., Hamerton, I., Jayawardena, K. D. G. I., Chen, J. S., Stolojan, V., et al. (2016). Multi-functional carbon fibre composites using carbon nanotubes as an alternative to polymer sizing. *Sci. Rep.* 6, 37334–37411. doi:10.1038/srep37334

Pradhan, S. S., Unnikrishnan, L., Mohanty, S., and Nayak, S. K. (2020). Thermally conducting polymer composites with EMI shielding: a review. *J. Electron Mater* 49, 1749–1764. doi:10.1007/s11664-019-07908-x

Prauchner, M. J., and Rodríguez-Reinoso, F. (2012). Chemical versus physical activation of coconut shell: a comparative study. *Microporous Mesoporous Mater.* 152, 163–171. doi:10.1016/j.micromeso.2011.11.040

Priya, D. S., Kennedy, L. J., and Anand, G. T. (2023). Emerging trends in biomass-derived porous carbon materials for energy storage application: a critical review. *Mater. Today Sustain.* 21, 100320. doi:10.1016/j.mtsust.2023.100320

Qin, F., and Brosseau, C. (2012). A review and analysis of microwave absorption in polymer composites filled with carbonaceous particles. *J. Appl. Phys.* 11, 061301. doi:10.1063/1.3688435

Raghavendra, N., Narasimha Murthy, H. N., Krishna, M., Vishnu Mahesh, K. R., Sridhar, R., Firdosh, S., et al. (2013). Mechanical behavior of organo-modified Indian bentonite nanoclay fiber-reinforced plastic nanocomposites. *Front. Mater Sci.* 7, 396–404. doi:10.1007/s11706-013-0224-6

Reddy, M. I., and Reddy, V. S. (2014). Dynamic mechanical analysis of hemp fiber reinforced polymer matrix composites. *Int. J. Eng. Res. Technol.* 3, 410–415.

Rezaei, F., Yunus, R., and Ibrahim, N. A. (2009). Effect of fiber length on thermomechanical properties of short carbon fiber reinforced polypropylene composites. *Mater Des.* 30, 260–263. doi:10.1016/j.matdes.2008.05.005

Saba, N., Jawaid, M., Alothman, O. Y., and Paridah, M. (2016). A review on dynamic mechanical properties of natural fibre reinforced polymer composites. *Constr. Build. Mater* 106, 149–159. doi:10.1016/j.conbuildmat.2015.12.075

Sallal, H. A. (2014). Effect of the addition coconut shell powder on properties of polyurethane matrix composite. *Al-Nahrain Journal for Engineering Sciences* 17: 203–210.

Singh, A. (2013). Study of mechanical properties and absorption behaviour of coconut shell powder-epoxy composites. *Int. J. Mater. Sci. Appl.* 2, 157. doi:10.11648/j.ijmsa.20130205.12

Song, P., Liu, B., Qiu, H., Shi, X., Cao, D., and Gu, J. (2021). MXenes for polymer matrix electromagnetic interference shielding composites: a review. *Compos. Commun.* 24, 100653. doi:10.1016/j.coco.2021.100653

Suchitra, M., and Renukappa, N. M. (2016). The thermal properties of glass fiber reinforced epoxy composites with and without fillers. *Macromol. Symp.* 361, 117–122. doi:10.1002/masy.201400227

Taurino, R., Bondioli, F., and Messori, M. (2023). Use of different kinds of waste in the construction of new polymer composites: review. *Mater. Today Sustain.* 21, 100298. doi:10.1016/j.mtsust.2022.100298

Thomassin, J. M., Jérôme, C., Pardoen, T., Bailly, C., Huynen, I., and Detrembleur, C. (2013). Polymer/carbon based composites as electromagnetic interference (EMI) shielding materials. *Mater. Sci. Eng. R Rep.* 74, 211–232. doi:10.1016/j.mser.2013.06.001

Ulus, H., Üstün, T., Sahin, Ö. S., Karabulut, S. E., Eskizeybek, V., and Avcı, A. (2016). Low-velocity impact behavior of carbon fiber/epoxy multiscale hybrid nanocomposites reinforced with multiwalled carbon nanotubes and boron nitride nanoplates. *J. Compos Mater* 50, 761–770. doi:10.1177/0021998315580835

Vilay, V., Mariatti, M., Mat Taib, R., and Todo, M. (2008). Effect of fiber surface treatment and fiber loading on the properties of bagasse fiber-reinforced unsaturated polyester composites. *Compos Sci. Technol.* 68, 631–638. doi:10.1016/j.compscitech.2007.10.005

Wang, L., Ma, Z., Zhang, Y., Chen, L., Cao, D., and Gu, J. (2021). Polymer-based EMI shielding composites with 3D conductive networks: a mini-review. *SusMat* 1, 413–431. doi:10.1002/sus2.21

Wang, Z., Wei, G., and Zhao, G. L. (2013). Enhanced electromagnetic wave shielding effectiveness of Fe doped carbon nanotubes/epoxy composites. *Appl. Phys. Lett.* 103, 1–6. doi:10.1063/1.4828356

Zeng, X., Cheng, X., Yu, R., and Stucky, G. D. (2020). Electromagnetic microwave absorption theory and recent achievements in microwave absorbers. *Carbon N. Y.* 168, 606–623. doi:10.1016/j.carbon.2020.07.028

Zhao, R., Xia, J., Adamaquaye, P., and Zhao, G. (2022). High density interfaces enhanced microwave absorption in multifunctional carbon nanotubes-glass fiber-epoxy composites. *Polym. Adv. Technol.* 33, 818–830. doi:10.1002/pat.5558

Zheng, Y., Ning, R., and Zheng, Y. (2005). Study of SiO2 nanoparticles on the improved performance of epoxy and fiber composites. *J. Reinf. Plastics Compos.* 24, 223–233. doi:10.1177/0731684405043552

Zhou, Y., Pervin, F., Rangari, V. K., and Jeelani, S. (2007). Influence of montmorillonite clay on the thermal and mechanical properties of conventional carbon fiber reinforced composites. *J. Mater Process Technol.* 191, 347–351. doi:10.1016/j.jmatprotec.2007.03.059